Southeast-Asian J. of Sciences: Vol. 1, No. 1(2012) pp. 101-112

THE FINITE-DIFFERENCE TIME-DOMAIN METHOD USING FOR MATERIAL COMPUTATION

Vu Ngoc Hai

Nguyen Tat Thanh University
300A Nguyen Tat Thanh Str., Dist. 4, Hochiminh City, Vietnam
e-mail: vnhai@ntt.edu.vn

Abstract

This is a report on an effective simulation method for analyses of optical material such as photonic crystal materials, Photonics Crystal Fibers... This method is based on the Finite Difference Time Domain (FDTD) algorithm. We observed the temporal dynamics of light waves in a bent fiber in a simulation, and obtained the electromagnetic fields as a function of optical wavelength for the commercial photonic crystal layer or fibers. The accuracy of this method was verified by good agreement between the simulation and experimental data.

1. Introduction

The Finite Difference Time Domain (FDTD) method is the formulation of Maxwells equations in the time domain and this method was introduced by K. Yee in 1966 [1]. Maxwells curl equations are discretized in space and time by approximating with centered two-point finite differences. The flexibility and capability of studying complex structures, easy implementation, visualizing the time-varying fields with the volume of space, handling nonlinear, frequency dependent, and conducting materials, obtaining easily broad spectral information by a single run made FDTD a powerful and versatile numerical tool. FDTD provides EM field variations in space with respect to time [2,3].

Theoretical studies of guided modes in PCFs have been performed based on a wide variety of techniques, which include the full vectorial effective index method, plane wave expansion method, finite element method, the localized basis function method, and the finite-difference time domain (FDTD) method [4].

In this paper, we study the FDTD technique for full analyses of microstructured or photonic crystal fibers. Compared with other techniques, the FDTD method has most simple and straightforward algorithm for solving time-dependent electromagnetic problems. The algorithm contains minimal assumptions and approximations and thus provides fairly reliable results as long as the spatial and temporal resolutions are high enough. Currently the FDTD technique is one of the most popular techniques for the study of the 3-dimensional photonic crystal structures such as nano-cavities and waveguides. There also have been a few reports on the 2-D FDTD method PCFs and the calculation of the elementary properties of PCFs were demonstrated.

Here we present the full aspects of FDTD technique modified for the analyses of photonic crystal fiber and demonstrate its wide range of capabilities. This paper will help understand the basic principles, optimization techniques, and learn how to apply this method for their own purposes. This paper, the basic algorithm of the modified FDTD method used in this study is summarized. The principle of Yee cell is introduced in the first part 2. The third part 3 will explain about basically formulation of 3D-FDTD. Phase matching layer, boundary condition, are described in detail in the part 4, 5. The conclusions of this chapter are in part 6.

2 Three Dimensional FDTD Algorithm

The FDTD method is based on an algorithm that calculates the temporal evolvement of the electromagnetic fields. Maxwells equation is solved at each discrete time by a so-called Yee-cell technique on a discrete three-dimensional mesh. In Yees, the grids for E and H fields are interleaved in the space and the positions of the electric and magnetic field components in a unit cell of the FDTD lattice in Cartesian coordinates as shown in Figure 1. In a 3-D case, each E component is surrounded by four H components and each H component is surrounded by four E components in computation. The adjacent field components are needed to generate another field component as time is marching. An arbitrary material object can be approximated by building up unit cells for which field component positions are disposed with the desired values of permittivity and permeability. Also, the arbitrary object may consist of different kinds of materials. Once the geometry of the object is specified in the calculation region, source condition is modeled somewhere in the region. Initially, it is assumed that all fields within the numerical simulation region are identically zero. Then, an incident wave is enforced to enter the simulation region. All the E components in the 3-D spaces are calculated first, and stored in memory for a particular time point using the H components previously stored in memory. Then all the H components are updated and stored in memory using the E data just computed. Therefore, the electric and magnetic field

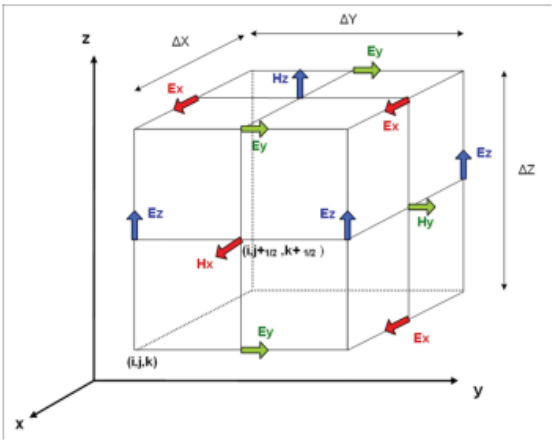

Fig. 1. Conventional Yees 3-D mesh.

components are evaluated at different time spots and at different grid points, shifted by a half period both in space and time. This process is repeated over multiple periods [3].

Let us first consider a region of space which is source-free and lossless. Using the MKS system of units, Maxwells curl equations are expressed as:

$$\nabla \times \mathbf{E} = -\mu \frac{\partial \mathbf{H}}{\partial t} \tag{1}$$

$$\nabla \times \mathbf{H} = \epsilon \frac{\partial \mathbf{E}}{\partial t} \tag{2}$$

where $\epsilon = \epsilon_r \epsilon_0$ is the electrical permittivity constant in farads/meter and is the magnetic permeability constant in henrys/meter. Assuming that ϵ and μ are scalar quantities (that is, the medium is assumed to be isotropic, linear, non-dispersive), expanding the curl expressions in (3-1), and equating the like components yields the following system of equations,

$$\frac{\partial H_x}{\partial t} = -\frac{1}{\mu}\left(\frac{\partial E_z}{\partial y} - \frac{\partial E_y}{\partial z}\right) \tag{3a}$$

$$\frac{\partial H_y}{\partial t} = -\frac{1}{\mu}\left(\frac{\partial E_x}{\partial z} - \frac{\partial E_z}{\partial x}\right) \tag{3b}$$

$$\frac{\partial H_z}{\partial t} = -\frac{1}{\mu}\left(\frac{\partial E_y}{\partial x} - \frac{\partial E_x}{\partial y}\right) \tag{3c}$$

$$\frac{\partial E_x}{\partial t} = \frac{1}{\epsilon}\Big(\frac{\partial H_z}{\partial y} - \frac{\partial H_y}{\partial z}\Big) \tag{4a}$$

$$\frac{\partial E_y}{\partial t} = \frac{1}{\epsilon}\Big(\frac{\partial H_x}{\partial z} - \frac{\partial H_z}{\partial x}\Big) \tag{4b}$$

$$\frac{\partial E_z}{\partial t} = \frac{1}{\epsilon}\Big(\frac{\partial H_y}{\partial x} - \frac{\partial H_x}{\partial y}\Big) \tag{4c}$$

The system of six coupled partial differential equations in (3) and (4) forms the basis for the FDTD analysis of electromagnetic wave interactions with general three-dimensional objects. It should be noted that the electric and magnetic field components (E_x, E_y, E_z, H_x, H_y, and H_z) are inter-related. Since these equations are functions of space and time, they can be discretized in the space and time domains and used to find field solutions numerically. Referring to Figure 1, we denote a grid point in the rectangular lattice as

$$(i, j, k) = (i\Delta x, j\Delta y, k\Delta z) \tag{5a}$$

and any function of space and time as

$$F^n(i, j, k) = F(i\Delta x, j\Delta y, k\Delta z, n\Delta t) \tag{5}$$

where $\Delta x, \Delta y$, and Δz are, respectively, the lattice space increments in the x, y, and z coordinate directions and Δt is the time increment, while i, j, k, and n are integers. Using central finite difference approximation for space and time derivatives that are accurate to second order, the partial derivatives are expressed as

$$\frac{\partial F^n(i, j, k)}{\partial x} = \frac{F^n(i + \frac{1}{2}, j, k) - F^n(i - \frac{1}{2}, j, k)}{\Delta x} + O(\Delta x^2) \tag{6a}$$

$$\frac{\partial F^n(i, j, k)}{\partial x} = F^{1+\frac{1}{2}}(i, j, k) - F^{n-\frac{1}{2}(i,j,k)}\Delta t + O(\Delta t^2) \tag{6b}$$

Applying (6) to the space and time derivatives in (3a), (3b), and (4c), we obtain the following FDTD approximation as representative relations in a three-dimensional FDTD formulation

$$\begin{aligned} H_x^{n+\frac{1}{2}}(i, j + \frac{1}{2}, k + \frac{1}{2}) &= H_x^{n-\frac{1}{2}}(i + \frac{1}{2}, j + \frac{1}{2}, k + \frac{1}{2}) \\ &+ \frac{\Delta t}{\mu}\Big\{\Big[\frac{E_y^n(i, j + \frac{1}{2}, k + 1) - E_y^n(i, j + \frac{1}{2}, k)}{\Delta z}\Big] \\ &- \Big[\frac{E_y^n(i, j + 1, k + \frac{1}{2}) - E_y^n(i, j, k + \frac{1}{2})}{\Delta y}\Big]\Big\} \end{aligned} \tag{7a}$$

$$H_x^{n+\frac{1}{2}}(i+\frac{1}{2},j,k+\frac{1}{2}) = H_x^{n-\frac{1}{2}}(i+\frac{1}{2},j,k+\frac{1}{2}) + \frac{\Delta t}{\mu}\Big\{\Big[\frac{E_z^n(i+1,j,k_{\frac{1}{2}}) - E_z^n(i,j,k+\frac{1}{2})}{\Delta x}\Big] - \Big[\frac{E_y^n(i+\frac{1}{2},j,k+1) - E_y^n(i+\frac{1}{2},j,k+1) - E_y^n(i+\frac{1}{2},j,k)}{\Delta z}\Big]\Big\} \tag{7b}$$

$$E_z^{n+\frac{1}{2}}(i,j,k+\frac{1}{2}) = H_x^{n-\frac{1}{2}}(i,j,k+\frac{1}{2}) + \frac{\Delta t}{\epsilon_0\epsilon_r(i,j,k+\frac{1}{2})}\Big\{\Big[\frac{H_y^n(i+\frac{1}{2},j,k+\frac{1}{2}) - H_y^{n+\frac{1}{2}}(i-\frac{1}{2},j,k+\frac{1}{2})}{\Delta x}\Big] - \Big[\frac{H_x^{n+\frac{1}{2}}(i,j+\frac{1}{2},k+\frac{1}{2}) - H_y^{n+\frac{1}{2}}(i,j-\frac{1}{2},k+\frac{1}{2})}{\Delta y}\Big]\Big\} \tag{7c}$$

It is understood from (7a) that H_x is located at $(i, j_{\frac{1}{2}}, k+\frac{1}{2})$ the H and E components are interleaved within the unit cell, and that the new value of a field vector component (H_x) at any lattice point depends only on its previous value and the previous values of the components of the other field vector at adjacent points. Then, the next computation of the field vector is continued as time is matching by a given time step.

It is generally assumed that fibers have no variations along the direction of propagation, and variations of material properties (such as refractive index) are limited to the transverse directions. Holey fibers that will be analyzed here are assumed to have geometries such that the refractive index is uniform along the z-axis. A schematic of a cross section of an example holey fiber is illustrated in Figure 2. Thus, instead of using a full-wave analysis based on (3) and (4) to numerically model the waveguide structures, we can take advantage of properties of the propagating modes to simplify the formulation. The components of electric and magnetic fields in waveguides with no variations along the direction of propagation (z-axis) can be expressed as

$$F(x,y,z) = F(x,y)e^{-j\beta z} \tag{8}$$

where β is the axial propagation constant. Using (3-8) and employing the notations of space and time in FDTD, the adjacent electric and magnetic fields in the axial propagation direction are related as

$$E^n(i,j,k\pm 1) = E^n(i,j,k)e^{\mp j\beta\Delta z} \tag{9a}$$

$$H^n(i,j,k\pm 1) = H^n(i,j,k)e^{\mp j\beta\Delta z} \tag{9b}$$

Now, the electric and magnetic fields become complex quantities based on phasor notations. The first-order partial derivatives with respect to z in the discretized space domain require two adjacent fields. The two adjacent fields can be represented by a field at the mid point between them. Furthermore, the first-order partial derivatives with respect to z in (3.3) and (3.4) are replaced with $-j\beta$, because the z-dependence of fields is as $\exp(-j\beta z)$. Based on these two facts, the following expressions are obtained,

$$\left\{\frac{E^n(i,j,k+1)-E^n(i,j,k}{\Delta z}\right\} = j\beta E^n(i,j,k+\frac{1}{2}) = -j\beta E^n(i,j,k)e^{-j\beta\frac{\Delta z}{2}} \tag{10a}$$

$$\left\{\frac{H^n(i,j,k+1)-H^n(i,j,k)}{\Delta z}\right\} = -j\beta H^n(i,j,k+\frac{1}{2}) = -j\beta H^n(i,j,k)e^{-j\beta\frac{\Delta z}{2}} \tag{10b}$$

Substituting the electric and magnetic field components from (10) into (7), we can establish the formulation system for 3D-FDTD which can calculate the electromagnetic propagation in fiber.

With above equation systems of finite difference expressions, the new value of an electromagnetic field vector component at any lattice point depends only on its previous value, the previous values of the component of the other field vector at adjacent points, and the known electric and magnetic current source. Therefore, at any given time step, the computation of a field vector can proceed either one point at a time, or, if p parallel processors are employed concurrently, p points at a time.

The optical pulse propagation along a fiber can be directly simulated if a computation structure includes a 3-dimentional piece of fiber of which length is much longer than the pulse width. Such a simulation requires enormous memory and computation time, making the FDTD method impractical in those cases. However, when considering continuous wave propagation along the fiber, both the electromagnetic wave and dielectric structure remain constant along the fiber length, with only exception of continuous increment of the optical phase. Therefore, the 3-dimentional fiber structure can be reduced to the one with arbitrary short length if a proper boundary condition is applied to count the optical phase difference along the length as show in next part.

3. Boundary Conditions

To truncate the computational region boundary conditions are required. They should absorb the out-going EM field by suppressing the spurious back reflected energy regardless of the polarization, propagation direction, and frequency. Absorbing boundary condition (ABC), perfectly matched layer (PML), or periodic boundary condition (PBC) are usually implemented with FDTD. Below I outline briefly the PML and PBC.

3.1 Perfectly Matched Layer

When an arbitrary electromagnetic object is analyzed numerically using FDTD, regions extending to infinity need to be modeled carefully. For example, in PCF analysis using FDTD, the center region is surrounded by very large cladding medium (usually silica). Modeling infinite media, whether they are modeled in one-, two-, or three-dimensional space, is practically impossible because of computer memory limitation even with the advanced current technology. This fact spells out the need for a special method to simulate regions extending to infinity. One way to model an infinite medium is to introduce an absorbing boundary condition (ABC) at the outer lattice boundary. Somehow, the outer boundary should be matched to an absorbing material medium. This is analogous to the physical treatment of the walls of an anechoic chamber. Ideally, the absorbing medium is only as thick as a few lattice cells, reflectionless to all impinging waves over their full frequency spectrum, highly absorbing, and effective in the near field of a source or a scattered.

In order to obtain a finite-sized calculation, the number of grid points should be finite. At the spatial boundaries of the calculation domain, the electromagnetic should satisfy condition such, that the space outside this domain in a desired way, e.g., a non-reflection continuation of the structure inside the calculation window. To make energy crossing the boundary not return inside the calculation window, usually a layer of absorbing material along the boundary is introduced. The best solution known is the induction of perfect matched layers (PMLs) that were introduced by Bérenger.

In 1994, Bérenger introduced a highly effective ABC, which is designated as perfectly matched layer (PML). The innovation of Berengers PML is that plane waves of arbitrary incidence, polarization, and frequency are matched at the boundary. For this, Berenger derived a novel split-field formulation of Maxwells equations where each vector field component is split into two orthogonal components. Each of the components is then expressed as satisfying a coupled set of first-order partial differential equations. By choosing loss parameters consistent with a dispersionless medium, a perfectly matched planar interface is established [5,6].

Particularly in our method, the computational domain is surrounded by a lossy material that absorbs the unwanted reflections such that the field is decaying exponentially inside the PML region. This method is just a mathematical model with no physical medium. The wave impedance is matched at the boundary between the computational domain and absorbing layer by splitting the field $H_z = H_{zx} + H_{zy}$ for TE and $E_z = H_{zx} + H_{zy}$ for TM and assuming $\frac{\sigma}{\epsilon} = \frac{\sigma^*}{\mu}$ where σ and σ^* are the electric and magnetic conductivity, respectively.

In the PML layer, exponential differencing has to be used because the field

decays quickly so linear differencing is not adequate. There may be a small reflection from this layer but the reflected field travels the PML region towards the computational domain and it is attenuated second time[7]. So if the PML layer thickness is large enough the back reflected field is usually very small in amplitude. The expressions for the boundary layers around the computational domain are

$$\begin{aligned} \epsilon\frac{\partial E_x}{\partial t} + \sigma_y E_x &= \frac{\partial H_z}{\partial y} = \frac{\partial (H_{zx} + H_{zy})}{\partial y} \\ \frac{\partial E_y}{\partial t} + \sigma_x E_y &= -\frac{\partial H_z}{\partial x} = -\frac{\partial (H_{zx} + H_{zy})}{\partial x} \\ \mu\frac{\partial H_{zx}}{\partial t} + \sigma_x^* H_{zx} &= -\frac{\partial E_y}{\partial x} \\ \mu\frac{\partial H_{zy}}{\partial t} + \sigma_y^* H_{zy} &= -\frac{\partial E_x}{\partial y} \end{aligned} \tag{11}$$

The formulation for TM case is similar to the TE one [8].

Figure 2 shows the cross section of a PCF is surrounded by PML region, where x and y are the transverse directions, z is the propagation direction. There is no PML in the upper and lower plane of PCF. The phase matching condition will be applied in these planes.

3.2 The Periodic 3D-FDTD Algorithm

Since the optical wave has no variation along the length except the phase in the above situation, the computation structure for the FDTD method can be reduced to one slice of the bent fiber with an arbitrarily small thickness.

The optical pulse propagation along a fiber can be directly simulated if a computation structure includes a 3-D piece of fiber whose length is much longer than the pulse width. Such a simulation requires enormous memory and computation time, making the FDTD method impractical in such cases. However, when considering continuous wave propagation along the fiber, both the electromagnetic wave and dielectric structure remain constant along the fiber length, with the exception of a continuous increment of the optical phase. Therefore, the 3-D fiber structure can be reduced to an arbitrarily short length if a proper boundary condition is applied to account for the optical phase difference along the length, as shown in Fig. 3.2. Now the electromagnetic fields at the boundary layers can be updated using the fields at the opposite boundary layer after applying this phase difference.

For minimum calculation time and memory requirements, the computational domain may include just one computation grid along the z-axis with a size of Δz, which makes it a (effectively) 2-D structure. The propagation constant β along the z direction is specified by the user, and the phase difference between the upper and lower boundaries of a unit grid is $\Delta\varphi = \beta\Delta z$. Here

we used both real and imaginary parts for E and H fields to define the optical phase. The absorptive layers are employed at the boundaries in the $x-y$ plane.

The optical variation (in phase or amplitude) along the z axis is usually much faster than those along the x and y axes, and thus a high grid resolution along the z-axis is essential for accurate simulation. Here we adopted anisotropic resolution along each axis to increase the resolution for the z-axis, while keeping the resolution along the x- and y-axes low to reduce memory requirements and computation time.

This approach is very similar to the 2-D FDTD method reported previously. The 2-D FDTD algorithm is definitely more compact than our 3-D case. However, it should be noted that our method retains the original 3-D FDTD algorithm, and thus it can handle both 3-D and 2-D structures without need of modification of the codes. (The boundary condition does nothing in the case of 3-D simulation since the absorptive layers are also imposed at the z-boundaries and the field intensities become zero.) Thus, it gives us greater flexibility compared to the 2-D FDTD method developed solely for 2-D waveguides or fibers [9].

4. Parameters and Stability

There are several parameters to choose for FDTD computer simulation of dielectric waveguides. First, appropriate computer memory size for calculation needs to be prepared. Basically, larger calculation matrix size will produce better accuracy. But if the matrix is too large, the required time for simulation will be unnecessarily too long. With proper size of the simulation region, size of PML should be considered. We need to make sure that the cell size is adequate for perfectly matching to the outer boundary. Then, parameters that define geometry and material properties of a waveguide need to be considered. They can be the core radius or refractive index of a step-index fiber, the cladding refractive index, or the side length if a fiber to be simulated has square core. Using the parameters to define the cross section, one can create any type of optical fiber. Finally, we need to choose a reasonable value for β. In other words, what we are trying to find in the FDTD simulation is the wavelength associated with the β value of the desired mode.

We have just seen that the choice of spatial resolutions $\Delta x, \Delta y, \Delta z$ and time resolution Δt can affect the propagation of numerical waves in Yee space lattice, and therefore the numerical errors. This part, we show that Δt must also be bounded to ensure numerical stability.

A stability limit is determined by choosing a suitable time step Δt to ensure the solutions with purely real frequencies for all the possible wave vector k to ensure the numerical stability of the above FDTD time step, the time step

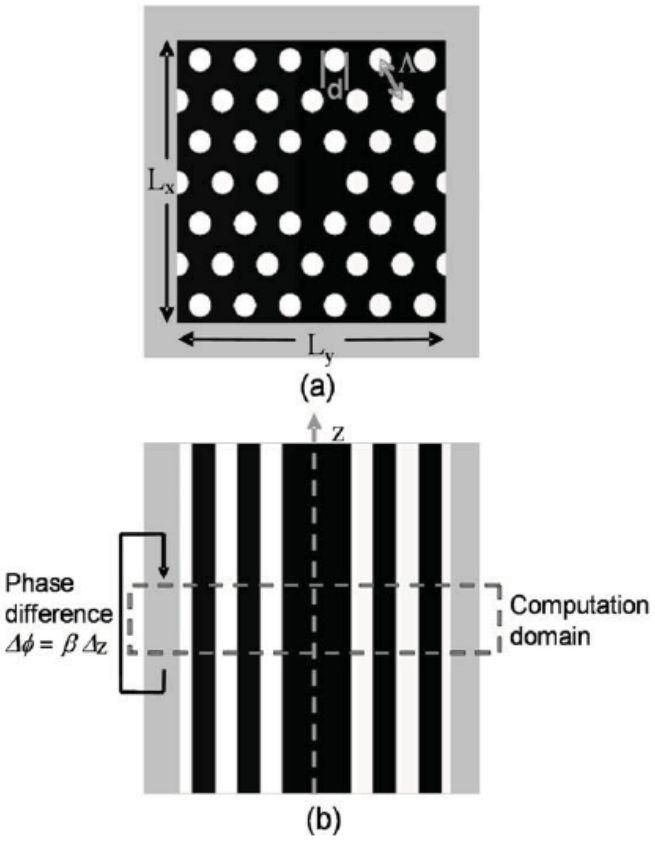

Fig. 2 The cross section in xy plane and xz plane of the computational domain. Black represents silica regions and white represents vacuum. The gray region on the edges denotes the phase match layer (PML).

should satisfy

$$\Delta t \leq \Delta t_{\max} = \frac{1}{c\sqrt{\frac{1}{(\Delta x)^2} + \frac{1}{(\Delta y)^2} + \frac{1}{(\Delta z)^2}}} \tag{12}$$

where c is the speed of the light.

5. Simulation Procedure

The simulation results we obtain from the FDTD computation are only electromagnetic field distributions. To extract certain information from the raw data, an interpretation step is required. Usually more than one simulation run is required to obtain desired information. In this section, we describe our simulation procedure and discuss how we interpreted the simulation results. The complete simulation procedure is as follows:

- Setup: the computation structure (geometry and grid sizes $\Delta x, \Delta y, \Delta z$); field excitation (location, center frequency, frequency bandwidth, and field polarization); propagation constant (β); and field-observation points are described in the setup file.

- Simulation: the E and H fields are computed and updated at each time step (T). Some of the field components are saved in storage for post-processing, as specified in the setup file.

- Post-processing: The stored field data are analyzed in the time, frequency, and spatial domains.

6. Conclusion

We proposed an efficient numerical method for bending analyses of optical material, especially Photonic Crystal Fiber, based on the FDTD. The time-domain simulation of the optical propagation in a fiber provided a view of the temporal dynamics of the optical field as well as the mode profile. The technique outlined here is directly applicable to not only PCFs, but also any kind of waveguides with arbitrary index profiles. It is important to note that this FDTD method can be easily extended by adding new functions to include nonlinear or strain effects in the simulation. We believe it is a useful tool for analyses and design of various micro-structured fibers

Acknowledgement This work was supported by the Regional Research Center for Photonic Materials and Devices, Chonnam National University, the Korea Research Foundation under Grant R08-2004-000-10503-0 and Nguyen Tat Thanh University. Many thanks to Prof. Nguyen Van Sanh for revision and review.

References

[1] X. Zhao, L. Hou, Z. Liu, W. Wang, G. Zhou, and Z. Hou, *Improved fully vectorial effective index method in photonic crystal fiber,* Appl. Opt. **46**(2007), 4052-4056.

[2] J. Arriaga, J. C. Knight, and P. St. J. Russell, *Modeling the propagation of light in photonic crystal fibers,* Physica D **189**(2004), 100106.

[3] F. Brechet, J. Marcou, , D. Pagnoux, P. Roy, *Complete analysis of the characteristics of propagation into photonic crystal fibers by the finite element method,* Opt. Fiber. Technol. **6**(2000), 181191.

[4] H. Uranus and H. Hoekstra, *Modelling of microstructured waveguides using a finite-element-based vectorial mode solver with transparent boundary conditions,* Opt. Express **12**(2004), 2795-2809.

[5] D. Mogilevtsev, T. A. Birks, and P. St. J. Russell, *Localized Function Method for Modeling Defect Modes in 2-D Photonic Crystals,* Journal of lightwave technology, Vol.17 , No. 11(1999), 2078-2081.

[6] Lou Shuqin, Wang Zhi, Ren Guobin, Jian Shuisheng, *An efficient algorithm for modeling photonic crystal fibers,* Optical Fiber Technology **11**(2005), 3445.

[7] A.Taflove, S. C.Hagness, "Computational electrodynamics: the Finite-Difference Time-Domain method", Artech House, 2005.

[8] M. Qiu, *Analysis of guided modes in photonic crystal fibers using the finite-difference time-domain method,* Microwave Opt. Technol. Lett. **30**(2001), 327330.

[9] J. P. Berenger, *A perfectly matched layer for the absorption of electromagnetic waves,* J. Comput. Phys., vol. **114**(1994), 185-200.